Energetics of Vesicle Fusion Intermediates: Comparison of Calculations with Observed Effects of Osmotic and Curvature Stresses

Vladimir S. Malinin* and Barry R. Lentz[†]

*Transave, Inc., Monmouth Junction, New Jersey 08852; and [†]Department of Biochemistry & Biophysics and Program in Molecular and Cellular Biophysics, University of North Carolina at Chapel Hill, Chapel Hill, North Carolina 27599

ABSTRACT   We reported previously the effects of both osmotic and curvature stress on fusion between poly(ethylene glycol)-aggregated vesicles. In this article, we analyze the energetics of fusion of vesicles of different curvature, paying particular attention to the effects of osmotic stress on small, highly curved vesicles of 26 nm diameter, composed of lipids with negative intrinsic curvature. Our calculations show that high positive curvature of the outer monolayer "charges" these vesicles with excess bending energy, which then releases during stalk expansion (increase of the stalk radius, r_s) and thus "drives" fusion. Calculations based on the known mechanical properties of lipid assemblies suggest that the free energy of "void" formation as well as membrane-bending free energy dominate the evolution of a stalk to an extended transmembrane contact. The free-energy profile of stalk expansion (free energy versus r_s) clearly shows the presence of two metastable intermediates (intermediate 1 at $r_s \sim 0 - 1.0$ nm and intermediate 2 at $r_s \sim 2.5 - 3.0$ nm). Applying osmotic gradients of ± 5 atm, when assuming a fixed trans-bilayer lipid mass distribution, did not significantly change the free-energy profile. However, inclusion in the model of an additional degree of freedom, the ability of lipids to move into and out of the "void", made the free-energy profile strongly dependent on the osmotic gradient. Vesicle expansion increased the energy barrier between intermediates by ~ 4 kT and the absolute value of the barrier by ~ 7 kT, whereas compression decreased it by nearly the same extent. Since these calculations, which are based on the stalk hypothesis, correctly predict the effects of both membrane curvature and osmotic stress, they support the stalk hypothesis for the mechanism of membrane fusion and suggest that both forms of stress alter the final stages, rather than the initial step, of the fusion process, as previously suggested.

INTRODUCTION

Membrane fusion is essential to cellular function and is critical to such medically important processes as neurotransmitter release and viral infection. For this reason, theoretical modeling of simple lipid bilayer fusion has attracted the attention of researchers for the last two decades (Chernomordik and Zimmerberg, 1995). This effort has expanded considerably during the past two years (Kozlovsky and Kozlov, 2002; Kuzmin et al., 2001; Lentz et al., 2002; Markin and Albanesi, 2002; May, 2002). One reason for this renewed interest is that, although there is still some disagreement (Bentz, 2000; Bonnafous and Stegmann, 2000), there is now reasonable consensus on a model for the rearrangements of lipids leading to fusion. This model derives from the original proposal that two bilayers brought into close contact can merge their contacting (*cis*) monolayers in a torroidal "stalk" that joins the outer or contacting leaflets of the two original bilayers (Markin et al., 1984). The distal (*trans*) monolayers of this structure are not merged, but form a bilayer that prevents free movement of soluble components between the trapped aqueous compartments (Fig. 1). The material properties of lipid mesomorphic phases have been used to estimate the free energy of the stalk intermediate state and thus part of the barrier that must be overcome to accomplish fusion (Siegel, 1993). Although the free energy of the stalk was originally overestimated (Siegel,

1993), more recent calculations have shown the stalk structure to be quite accessible (Kozlovsky and Kozlov, 2002; Kuzmin et al., 2001; Markin and Albanesi, 2002; May, 2002). Indeed, a stalk structure is actually predicted to be stable (Markin and Albanesi, 2002) under certain circumstances, and such a structure has been observed as a stable lipid phase for diphytanoyl phosphatidylcholine (Yang and Huang, 2002). Early qualitative statements of the stalk hypothesis acknowledged the possible existence of other intermediates (Leikin et al., 1987). The free energy of a second possible type of intermediate in which distal monolayers pucker inward and touch (the transmembrane contact (TMC); Fig. 1) has also been estimated based on lipid material properties (Siegel, 1999). Another possible type of fusion intermediate results from radial expansion of the TMC. This is termed a "hemifusion diaphragm" or expanded TMC (ETMC) (Fig. 1). The existence of more than one type of intermediate has been kinetically observed only for poly(ethylene glycol) (PEG)-mediated fusion of imperfectly sonicated small vesicles (Lee and Lentz, 1997a), with more highly curved vesicles fusing under some circumstances according to a biexponential time course that also implies two intermediates (Evans and Lentz, 2002). The cause of this apparent variability of mechanism is not clearly understood, although it should lie in the relative free energies of and the barriers between the presumed intermediates.

In this article, we estimate the free energy of the presumed fusion intermediates from lipid material properties as we continuously evolve these structures by radial expansion from a stalk toward the TMC and ETMC. Since the current
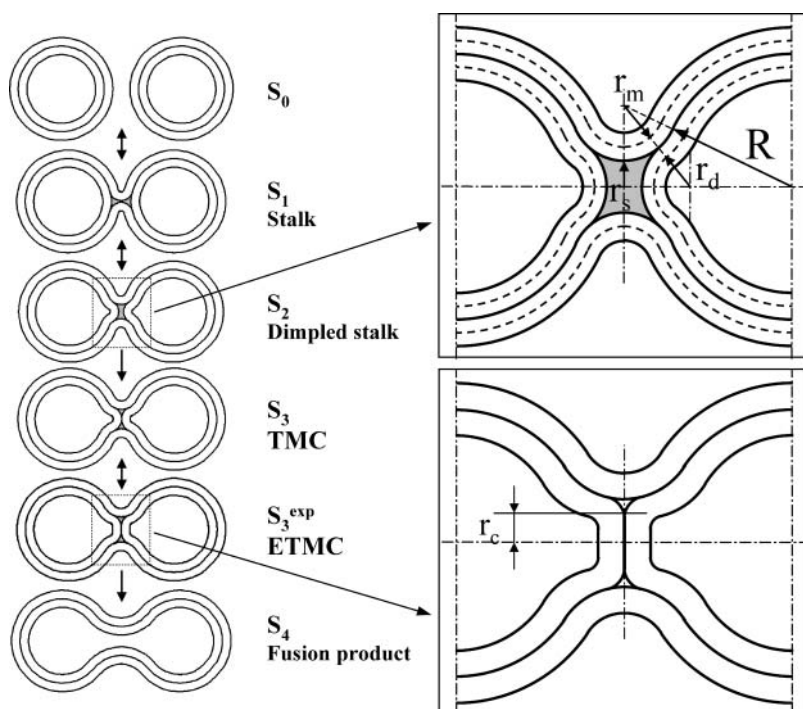
FIGURE 1 Model for membrane reorganizations presumed to be involved in the evolution of fusion intermediates. Vesicles are drawn to scale such that the vesicle radius to the interleaflet plane (R) is 11 nm, with the thickness of each monolayer taken as 2 nm, making the outer diameter 26 nm. The stalk radius (r_S) is the distance between the stalk axis and the apparent inner surface of the stalk (see *upper inset* at *right*). The marginal radius (r_m) and the dimple radius (r_d) are the radii of curvature of the indicated surfaces (*upper inset*). The sequential stages of the fusion process as presented are based on the stalk hypothesis. In this study's version of the stalk hypothesis, we assume that the evolution of lipidic structures leading to fusion involves two discontinuous events ($S_o \rightarrow S_1$, $S_3^{exp} \rightarrow S_4$) and a continuous change in structures as the stalk radius, r_S, increases from S_1 to S_3^{exp}. Stages in this process are S_o, separate vesicles; S_1, stalk; S_2, dimpled stalk (the stalk expands and the inner leaflets dimple but do not come into contact); S_3, *trans*-monolayer contact (TMC); S_3^{exp}, expanded TMC (ETMC) or diaphragm; and S_4, the final fusion product. Another parameter, r_c, the diaphragm radius, is needed to describe the ETMC (*lower right inset*). Note that the discontinuous first and last steps are not treated here (see text). Double arrows represent reversible processes. Hydrophobic mismatch or ''void'' region is shown as shaded area.

version of the stalk hypothesis presumes that the stalk evolves to a fusion pore by a similar process, we have used this calculation to judge whether observed effects of osmotic stress and membrane curvature on PEG-mediated vesicle fusion are consistent with the stalk hypothesis. Two major contributions to the free energy of fusion intermediate states have been proposed: 1), that associated with bending planar monolayers into torroids (bending energy), and 2), that associated with the inability of required nonlamellar structures to be described in terms of smooth torroids without producing hydrophobic ''voids''. The ''void'' energy was, in the initial approximation, taken as proportional to the surface area of the interface between lamellar structures and a hypothetical ''void'' that represented the space unfilled by uniformly packed monolayers continuously bent to match the hypothesized nonlamellar stalk structure (Siegel, 1993). A new form of membrane deformation has been proposed, which adds ''tilt'' of the hydrocarbon chains of lipid molecules to bending of the membrane surface, and a theory for this elastic model has been developed (Kozlovsky and Kozlov, 2002). This treatment allows for structures with discontinuous surfaces that can eliminate the ''void'' and provides an alternative to the hydrophobic ''void'' model for estimating the energy of nonlamellar structures associated with fusion intermediates. Both approaches to the problem of matching nonlamellar to lamellar lipid organization are equally valid and indeed are parameterized against the same experimental studies of lamellar to hexagonal phase transitions (Lentz et al., 2002). However, the ''void'' approach has the dual advantages for

our purposes of 1), simple parameterization in terms of a volume that must somehow be occupied with mass either from lipid molecules or from other bilayer components, and 2), formal consistency with the approach we have taken of treating bilayer bending in terms of continuously varying surfaces.

The macroscopic approaches described above are all clearly simplifications, but, if properly parameterized, they represent a useful first-order approach to the difficult problem of estimating the free energies of presumed intermediates on the path to fusion. All suffer from the same simplifying approximations, namely, 1), that molecular scale processes can be described by the macroscopic properties of continuous materials, and 2), that the bending free energy of highly curved intermediates can be described in a linearized approximation. Because of the first approximation, we limit our attention to steps in the fusion process that do not involve discontinuous changes in topology and thus gross reorientations of individual lipid molecules. We feel that such events are properly described only by stochastic treatments of groups of molecules or molecule-like particles. To test whether our treatment could reasonably model the highly curved, nonlamellar structures presumed to exist in fusion intermediates, we have examined published experimental data on the radius of hexagonal H_{II} phase cylinders of dioleoyl-phosphatidylethanolamine (DOPE) under osmotic stress (Leikin et al., 1996). The ability of our methods to account for the behavior of highly curved hexagonal cylinders (radii from ~2.8 nm to as small as ~1.75 nm) is documented in an accompanying Letter to the Editor

(Malinin and Lentz, 2004), and provides evidence that bending energy in Helfrich's form can be used for such bending deformations.

An equally significant approximation is that such calculations to date have treated fragments of flat bilayers rather than enclosed membrane structures with limited volume and membrane surface area. It is such structures whose fusion is generally studied experimentally. Fusion of membrane-enclosed compartments (vesicles) differs in many ways from fusion of flat membranes. First, high positive curvature of the outer monolayer, especially in the case of small vesicles, provides additional energy that can be released during stalk expansion or pore formation. Many experimental studies have shown that positive curvature stress promotes fusion (Lentz et al., 1987; 1992; Schmidt et al., 1981; Suurkuusk et al., 1976; Talbot et al., 1997; Wilschut et al., 1981), and there is experimental evidence that it is important at the point of biomembrane fusion (Kanaseki et al., 1997). It has been proposed that the local bending at the top of the dimples created by folding fusion protein machines may promote viral (Kozlov and Chernomordik, 1998) and synaptic (Lentz et al., 2000) fusion. The energy of an initial stalk formed between two opposite spherical ''nipples'' of radius 10 nm has been determined to be ~40 kT less than the energy of stalk formation between two flat membranes (Kuzmin et al., 2001). The second way in which vesicle geometry, as compared to a planar membrane geometry, alters the fusion process is that it applies restrictions on changes in each monolayer surface area, which in turn are linked to the change of internal volume and thus to osmotic conditions. This latter fact is of special interest for us. In a previous study, we observed unexpected effects of osmotic gradients on PEG-mediated fusion of small unilamellar vesicles (SUVs) (Malinin et al., 2002). We proposed that these unexpected effects of osmotic stress on membrane fusion might result from the ability of osmotic gradients to impede or encourage movement of lipids into hydrophobic ''voids'' created during the fusion process. Here we demonstrate that a simple modification of the stalk model can explain the observed effects of osmotic stress.

MODEL

Geometry

We limit our attention here to the intermediate steps of fusion of two spherical bilayer vesicles beginning from the formation of an initial stalk, through its radial expansion but before pore opening. The initial step in the fusion process (stalk formation) as well as the final step (pore formation) both involve discontinuities in system topology that we do not believe can be modeled adequately by the type of macroscopic materials approach used here to model intermediate evolution. As in the treatment of Siegel (1993), lipid monolayers in the intermediates are assumed to form surfaces that are segments of spheres or of spherical torroids. The thickness of monolayers, h, is held constant and equal to 2 nm. The vesicle radius, R, is defined as the distance from the center of the sphere to the intermonolayer surface (see Fig. 1). Obviously, when the vesicle bilayer is under elastic stress, the vesicle radius will change. Although the vesicle radius is not assumed to be constant

under elastic stress, the total number of lipid molecules composing the vesicle is held constant. We acknowledge this by defining the original radius R_o as the imaginary radius that a vesicle with a given number of lipids would have in the absence of elastic stress. R_o was usually 11 nm (if not indicated otherwise), consistent with the outer vesicle diameter of 26 nm ($2R_o + 2h$) that we have observed in experiments with SUVs (Malinin et al., 2002). R and two other geometrical parameters (r_m, stalk marginal radius, and r_d, dimple radius of curvature; Fig. 1) were not predefined to any particular values but allowed to vary to find the minimum of the free energy at each stalk radius (r_s, Fig. 1). For this reason, the stalk is not a simple spherical torroid with fixed assumed radii, but is optimized to minimize the stalk energy at each stalk radius. An analogous approach has been used to minimize stalk free energy by minimizing the stalk-bending deformation in the case of two fusing planar monolayers forming a surface of revolution with constant mean curvature (Markin and Albanesi, 2002). In our model, which includes multiple free energy components and more complex monolayer shapes, we could not minimize the free energy of the stalk by such a procedure. We used a conventional spherical-torroidal geometry, but varied the above-mentioned radii to minimize the total, not just bending energy. This lowered the total free energy significantly compared to the unrelaxed geometry. Global minimization of the free energies of lipid assemblies with respect to R, r_m, and r_d was performed with Mathematica 4.0 (Wolfram Research, Champaign, IL) using equations and parameters given below. The change of the total energy was calculated relative to the energy of a pair of nonfused but contacting vesicles at a given osmotic gradient.

The total free-energy change is modeled as a composite of six terms: the elastic membrane energy composed of a ''stretching/compression'' term (G_s) and a bending term (G_b), osmotic energy (G_{os}), ''void'' (hydrophobic mismatch) energy (G_v), hydration repulsion energy (G_h), and depletion energy (G_d).

$$\Delta G_{total} = \Delta G_s + \Delta G_b + \Delta G_{os} + \Delta G_v + \Delta G_h + \Delta G_d. \quad (1)$$

The elastic energy also contains a mixed stretching-bending term, which is assumed to be negligible. As pointed out previously (Kozlov and Winterhalter, 1991), this term is exactly zero if integration is carried out over a ''neutral surface'' for which the cross stretching-bending modulus is zero. Each of the terms introduced above was estimated as described below.

The elastic energy of membrane stretching/compression is defined as

$$G_s = \frac{1}{2} K_e (A_{in} \alpha_{in}^2 + A_{out} \alpha_{out}^2), \quad (2)$$

where A is the area of a monolayer, $\alpha = (A - A_o)/A_o$ is the relative area change of a monolayer, and K_e is the elastic expansion modulus of a monolayer. A_o is the area of a monolayer in the original unfused vesicle. The area is calculated for each leaflet over the neutral surface of the inner (*in*) or outer (*out*) monolayer. The neutral surface, at which bending and compression deformations occur independently, was assumed to locate 0.7 nm from the hydrophilic surface of the monolayer (Fuller and Rand, 2001) (or $h1 = 1.3$ nm from the hydrophobic surface). Thus, A_{in} and A_{out} were calculated as the area of spheres of radius $R - h1$ and $R + h1$, correspondingly.

The area expansion modulus for a dioleoyl-phosphatidylcholine (DOPC) bilayer is expected to be between the known values for the minimally unsaturated lipid 1-stearyl, 2-oleoyl-phosphatidylcholine (SOPC) (193 mN/m) and highly unsaturated diaracadonyl-phosphatidylcholine (135 mN/m) (Needham and Nunn, 1990). 1-Palmitoyl-2-oleoyl-phosphatidylethanol-amine (POPE) and cholesterol at a moderate concentration of 25 mol % slightly increase the expansion modulus (Evans and Needham, 1987; Needham and Nunn, 1990). These values allowed us to estimate K_e for a DOPC/POPE/Ch (cholesterol) (2:1:1) bilayer, the composition we used for osmotic gradient experiments (Malinin et al., 2002), to be nearly 200 mN/m, and for a monolayer 100 mN/m or 24.3 kT/nm^2.

The bending energy in general form (correct to second order) as introduced by Helfrich (1973) is defined as

$$G_b = \frac{1}{2} K_b \int_A \left(\frac{1}{R_1} + \frac{1}{R_2} - C_o \right)^2 dA + K_G \int_A \frac{1}{R_1} \frac{1}{R_2} dA, \quad (3)$$

where K_b and K_G are the bending elastic modulus and Gaussian curvature modulus of the monolayer, respectively; R_1 and R_2 are the principal radii of curvature (evaluated at the neutral surface of each monolayer); and C_o is the intrinsic curvature of the monolayer. As the bending energy is one of the most important terms in our calculation, exact material parameters (K_b, K_G, and C_o) could be crucial for our calculations. We used C_o values obtained by Chen and Rand (1997) from x-ray diffraction measurements of inverted hexagonal phases as ~ -0.17 nm^{-1} for DOPC/Ch (3:1) and ~ -0.37 nm^{-1} for DOPE/Ch (3:1) mixtures. Using the method of estimating molecular packing parameter proposed by Marsh (1996) and taking geometrical data for lipids from Chen and Rand (1997), we estimated the intrinsic curvature for our lipid composition DOPC/DOPE/Ch (2:1:1) as -0.23 nm^{-1}. Similarly, we used K_b values of 9 kT for DOPC/Ch and 15 kT for DOPE/Ch (Chen and Rand, 1997). Assuming that the inverse bending modulus is a weighted average of the inverse bending moduli of the individual components (Markin, 1981), we obtained $K_b \approx 11$ kT for DOPC/DOPE/Ch (2:1:1).

We did not have a reliable value for the Gaussian curvature modulus due to a lack of experimental data. According to a theoretical model proposed recently (Templer et al., 1998), the value of the ratio of the Gaussian curvature modulus to the mean curvature bending modulus (K_G/K_b) is restricted to $-1 < K_G/K_b < 0$. The integral of the Gaussian curvature over a closed surface always leads to a constant that depends only on the topology of the surface (do Carmo, 1976). This equals 4π for a sphere. Thus, the Gaussian curvature energy of the intermediates with different stalk radii but the same topology would be the same, and ignoring this term in Eq. 3 should not change the relative total free energy of intermediate states as a function of the stalk radius. Nevertheless, we have to keep in mind that the transitions from separate vesicles to the stalk and from the transmembrane contact (TMC; Fig. 1) to the fusion pore involves a topological change and hence a jump in the Gaussian free energy by $-4\pi K_G$ (increase in energy, since $K_G < 0$).

The bending energy as expressed in Eq. 3 is a sensitive function of area. Because membrane monolayers experience both area change and bending, as in our current model, we had to normalize the bending energy by integrating over the initial area (A_0) at the neutral plain (Kozlov and Winterhalter, 1991). In previous calculations of stalk free energy (Kozlovsky and Kozlov, 2002; Markin and Albanesi, 2002; Siegel, 1993, 1999), this was feasible since these calculations considered stalk formation between very large planar bilayers with constant area per molecule. In fusion of closed vesicles of finite size, as considered here, each monolayer undergoes geometrical changes during stalk formation and expansion. We cannot integrate bending energy literally over the initial area for such structures consisting of segments with different curvatures. Instead, we calculate bending energy for separate pieces as small as single molecules over the initial area assuming that the area change associated with formation of fusion intermediates is equally distributed over all lipid molecules. Then we can write

$$G_b = \sum g_{bm} = \frac{A_o}{A} \sum g_{bm} \frac{a_m}{a_{m0}} = \frac{A_o}{A} \sum \frac{1}{2} K_b \left(\frac{1}{R_{1i}} + \frac{1}{R_{2i}} - C_o \right)^2 a_m$$

$$= \frac{1}{2} K_b \frac{A_o}{A} \int_A \left(\frac{1}{R_1} + \frac{1}{R_2} - C_o \right)^2 dA. \quad (4)$$

In this expression, $g_{bm} = \frac{1}{2} K_b ((1/R_{1i}) + (1/R_{2i}) - C_o)^2 a_{m0}$ is the bending energy of ith molecule over the initial area of that molecule, a_{m0}, and a_m is the current area per molecule. The integration in the final expression on the right is over the current area (A), and we use a correction factor of A_o/A that

accounts for the neutral plane area change per molecule associated with forming a given structure.

The osmotic energy (the energy required to move water molecules in or out of vesicles to accommodate internal volume change) is defined as

$$\Delta G_{os} = -(\Pi_{in} - \Pi_{out}) \Delta V_{in}, \quad (5)$$

where V_{in} is the trapped volume, and Π_{in} and Π_{out} are the osmotic pressures inside and outside of vesicles, respectively. Here we assume that the membrane is impermeable to solutes, water is an uncompressible solvent, and the vesicle internal volume change is small. The latter approximation is good for small unilamellar vesicles. Thus, Π_{in} can be treated as a constant. We have not investigated the effect of osmotic gradient on fusion of large unilamellar vesicles.

The hydrophobic mismatch or "void" energy

In addition to the contributions outlined thus far, there is clearly additional energy associated with the mismatch of the bent monolayers associated with formation of nonbilayer intermediate lipid structures as shown in Fig. 1. To estimate this energy, our calculation takes an approach similar to that originally proposed by Siegel (1993) in treating the hexagonal phase in that it treats mismatch in terms of imaginary "voids" between the hydrophobic surfaces of monolayers of circular cross section (Siegel, 1993; Turner and Gruner, 1992). An alternative approach to treating the hexagonal phase is to assume a hexagonal cross section and to estimate this energy in terms of the "tilt" of lipid acyl chains needed to conform to this hexagonal geometry (Hamm and Kozlov, 1998). This approach has also been applied to calculating the free energy of presumed fusion intermediates (Kozlovsky et al., 2002). Of course, actual voids will not exist and processes other than chain tilt will contribute to satisfying the interstice strain. In reality, the normal lamellar lipid organization will distort to reduce hydrophobic mismatch, and this distortion may involve tilt, stretching of acyl chains (Kirk et al., 1984), or other local changes in phospholipid packing. Since none of these effects can be calculated rigorously based on first principles and must be parameterized by comparison to experiments, we prefer the simpler treatment of grouping these contributions into one term, and we treat all these deviations away from lamellar behavior in terms of the energy of the "void". Unlike Siegel (1993), we presume that this added unfavorable free energy should be proportional to the volume (not the surface) of the space left unfilled when we treat the bilayer leaflets as lamellar structures of uniform curvature, i.e., the volume of the "void". We base this assumption on two possible approaches that can be used to estimate the "void" energy. The first approach derives from consideration of "void" as a separate phase contacting the hydrophobic part of a monolayer and thus having additional surface energy. Since the distance between these surfaces in fusion intermediates is very small (in the range of 0–$\sim$1 nm), their surface tension is a function of this distance (Israelachvili and Pashley, 1982). Obviously, surface tension varies from 0 at distance 0 to the maximum "bulk" value at a distance much greater than the characteristic length of interaction between hydrophobic surfaces. It has been shown that this characteristic length is rather large, $\sim$10 nm (Israelachvili and Pashley, 1982). Thus, we can assume in our case that surface tension is proportional in the first order to the distance between void surfaces. So the total surface energy of "void" is calculated as the surface area of the lamellar-"void" interface times the tension of this interface and becomes proportional to the volume of "void". The second justification uses a molecular description of the nonlamellar structures of interest. In this approach, one can imagine that the work that must be done to extend acyl chains from the lamellar leaflets to occupy the nonlamellar "void" is also proportional to the distance between the center of the "void" and the "void"-lamellar interface. Since the number of chains that must be extended is proportional to the surface area of the interface between lamellar leaflets and "void", the free energy of the "void" is still proportional to its volume. Thus, we assume that the interstice energy in

fusion intermediates is to a first-order approximation proportional to the "void" volume

$$G_v = K_v V, \qquad (6)$$

where $K_v = 2.1$ kT/nm^3 is an empirical coefficient estimated as described below.

Two estimations for the free energy of a "void" have been reported in the literature, both based on the thermodynamics of the transition from lamellar to hexagonal phase in DOPE. Siegel (1993) has made an analysis of the free energy of the H_{II} phase of DOPE at 22°C that was based on essentially the same description of uniformly curved lamellar lipid arrangements as we have given above. He estimated the energy of a unit length of "trilaterally symmetric void" (TSV, see Fig. 2 A) as 10.5 kT/nm (Siegel, 1993). From the geometry of this structure, we find the cross-sectional area of the DOPE TSV $A_{TSV} = 2.56$ nm^2, thus obtaining specific interstice energy per unit volume 10.5:2.56 = 4.1 kT/nm^3. Using a similar approach, Kozlov et al. (1994) obtained for the interstice energy per lipid molecule a value of 0.35 kT, from which we calculated the energy per unit volume as ~2.1 kT/nm^3. The difference between these two estimates derives mostly from different values of the bending modulus used by these two authors. Kozlov et al. used a bending modulus of 10.2 kT, which is more consistent with the value used in our model (11 kT) than with that used by Siegel (20.7 kT). Thus, we use 2.1 kT/nm^3 for the "void" free energy. In a companion article, we have used the methods described here to estimate the void energy from the reported variation of DOPE hexagonal phase dimensions with osmotic stress (Leikin et al., 1996) and obtained the same value (Malinin and Lentz, 2004). This value is valid for a pure DOPE membrane. DOPC has the same acyl chains but a larger headgroup cross section, which creates additional restrictions for stretching acyl chains and should raise the "void" free energy. The presence of cholesterol in our membranes probably would lower the "void" free energy (see Discussion).

One can criticize our treatment of the void free energy as a linear function of the void volume. One of the ways to test this approach, as suggested by a reviewer, would be to fit published data for the effect of osmotic stress on the hexagonal unit size of DOPE (Leikin et al., 1996) to the hexagonal unit size predicted at each osmotic pressure based on the model including a contribution from the "void". This has the advantage both of first validating our model with experimental results on nonlamellar structures and of providing a set of energy parameters obtained in a fashion consistent with the assumptions in our model. The parameter values thus obtained (Malinin and Lentz, 2003) were $1/R_{0p} = -0.32$ nm^{-1}, $K_b = 11$ kT, and $K_v = 2.0$ kT/nm^3, which are very close to the conventional estimates ($1/R_{0p} = -0.35$ nm^{-1}, $K_b = 11$ kT, and $K_v = 2.1$ kT/nm^3).

Hydration repulsion energy

Membrane surfaces approach each other quite closely in some of the intermediates (see Fig. 1), e.g., between opposite outer leaflets at early stalk (small marginal radius, r_m) or between inner surfaces of the inner dimple at early TMC (small dimple radius, r_d). This required that we take into account the repulsive pressure between these closely opposed monolayers. Repulsion between flat parallel bilayers dominates at separations $< \sim 20$–30 Å and is well described by a single exponential of the distance of approach, d_w, (Lis et al., 1982; Marra and Israelachvili, 1985):

$$P_r = P_0 \exp(-d_w/\lambda), \qquad (7)$$

where P_o is a preexponential factor, λ is the characteristic length of the repulsion, and d_w is the distance between membrane surfaces. The total repulsion pressure arises mainly from hydration repulsion, bending undulations, and protrusions of lipid molecules (McIntosh et al., 1995). The free energy of repulsion can be calculated by integrating the repulsion pressure over the distance between two membranes when they are brought from infinity to the distance d_w. In our case, membrane surfaces are not flat and parallel, and the exact solution can be obtained only within a particular physical model with known energy functional. To simplify, we drew a plane of symmetry between opposite membranes, and considered the distance from the membrane surface to the plane as a half distance between membranes (see Fig. 2 B). Thus, the energy of repulsion was defined as

$$G_h = \frac{1}{2} P_0 \lambda \int_A \exp(-2d_n/\lambda) dA, \qquad (8)$$

where d_n is the distance normal from the membrane surfaces to the surface equidistant from opposed membranes (Fig. 2 B). Integration was taken over the surfaces of close approach as mentioned above. For the parameters P_o and λ, we used published values for SOPC: $10^{10.5}$ dyn/cm^2 and 0.198 nm, respectively (Rand et al., 1988). POPE at a moderate concentration (<50 mol %) had little effect on the hydration properties of SOPC bilayers (Rand et al., 1988), so we can expect the same for the influence of DOPE on DOPC bilayers. The contribution of van der Waals attraction to the energetics of fusion intermediates should be negligible and thus was excluded from our calculations. This estimation of the hydration energy is very simplified. Nevertheless, this term accounts for only ~0.8 kT of free energy in the original state of a pair of aggregated vesicles, and accounts for an even smaller contribution to the energy of intermediate structures. Thus, the error
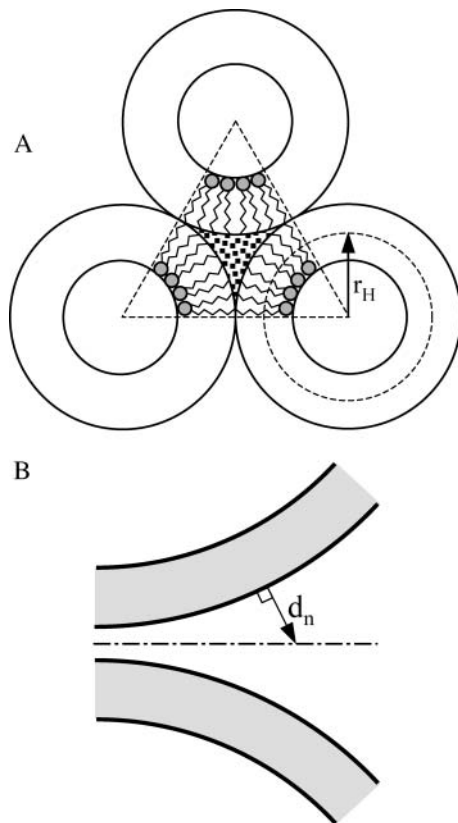

FIGURE 2 (A) Illustration of the trilaterally symmetric void (TSV) formed between hexagonal phase units (Siegel, 1999). r_H is the single leaflet radius of curvature in the hexagonal phase. B illustrates the geometrical parameter, d_n (the distance normal from the bilayer surfaces to the plane of equidistance between the bilayers), used to calculate the repulsion interaction between two membranes.

associated with using the approximate form probably does not exceed 0.1 kT and affects mainly the original energy.

Depletion energy

Because we meant for our calculations to model the behavior of vesicles aggregated and fused under the influence of PEG, we needed to account for changes in the depletion energy during the evolution of fusion intermediates. Depletion energy is the energy associated with exclusion of PEG from a layer of solvent near the membrane surface. As vesicles aggregate and fuse, the volume of the depletion layer (and thus the depletion energy) decreases. Assuming the simplest case ([PEG] = 0 at $x < L_d$, and [PEG]$_{bulk}$ at $x > L_d$) we obtain for the depletion energy

$$G_d = V_d \Delta \Pi_{PEG}, \qquad (9)$$

where L_d and V_d are the thickness and the volume of the depletion layer, respectively, $\Delta \Pi_{PEG}$ is the difference of osmotic pressure between the depletion layer (buffer) and the bulk (buffer + PEG), and x is the distance from the membrane surface. The volume V_d is calculated by integrating the depletion layer over the vesicle surfaces excluding intersecting volumes for the layers from the opposite membranes. The relative osmolality for 10 wt % PEG in our fusion buffer was measured as 93 mOs/kg, which corresponds to an osmotic pressure $\Delta \Pi_{PEG}$ of 2.32×10^5 N/m². L_d was taken as 1.5 nm (Arnold et al., 1990; Kuhl et al., 1996).

RESULTS AND DISCUSSION

Original state

We calculated the energy change after stalk formation and expansion relative to the energy of a pair of unfused vesicles. This makes it very important to define what is the unfused vesicle original state. We consider two definitions. First, to estimate the original area of each leaflet and the original internal volume, we considered unstressed vesicles of a particular radius R_o ("original state 0"). This is an imaginary state with no membrane stress. In reality, membranes of small vesicles are highly stressed. High bending energy of small vesicles tends to redistribute among other types of elastic energy, particularly energy of membrane stretching/compression. Since, in our calculations of the energy of fusion intermediates, we allowed the vesicle radius to vary, it is reasonable to assume that it is not fixed in the original state as well. Indeed, a slight increase in vesicle radius (decrease in geometrical curvature) will reduce bending energy but increase stretching energy. At some radius, there will be an optimal balance between stretching and bending energy with a minimum of total energy. This scenario we call "original state 1".

Since the inner leaflet of an SUV has high negative curvature and the outer leaflet has high positive curvature, the total bending energy of "state 1" can be reduced by a small redistribution of lipids between the inner and the outer leaflet. The extent and direction of redistribution will depend on the intrinsic curvatures of the lipids comprising the membrane. For example, moving negative curvature lipids from the positively curved outer leaflet to the neg-

atively curved inner leaflet can significantly reduce bending energy. Lipid redistribution can occur with or without a change in the lipid composition of each leaflet. The state that results from a redistribution of lipid mass between leaflets in "state 1" without a change in lipid composition of either leaflet will be called "original state 2". Correspondingly, "original state 3" is reached by a change in vesicle radius (as in "state 1") plus individual lipid redistribution resulting in different lipid compositions of the two leaflets. Whereas the first type of energy relaxation occurs instantly, the second and third ones (lipid flip-flop) may require a long relaxation time unless it is forced by sonication during vesicle formation. The correct choice of a reference state for our calculations depends on the exact mechanism of vesicle formation, which no one clearly understands.

We tested scenarios 1 and 2 for the original state for SUVs ($R_o = 11$ nm) composed of DOPC/DOPE/Ch 2:1:1 (intrinsic curvature $= -0.23$ nm^{-1}). The energy minimization leading to original "state 1" results in an increase in vesicle radius by 0.37%, with the relative expansion of the inner leaflet being 0.85% and that of the outer leaflet being 0.67%. Though these numbers do not look very large, the resulting outer leaflet stress may affect stalk formation. For reference, membrane rupture occurs when membranes expand by only ~4–5%. The total free energy of a pair of "state 1" vesicles, compared to the energy of a planar bilayer made of the same number of lipid molecules, in this state is 1432.3 kT, of which 4.1 kT is stretching/compression energy and the remaining 1428.2 kT is bending energy.

In "state 2", for the vesicles modeled here, the minimum of the free energy is reached when vesicle radius increases by 0.45% relative to R_o and the relative expansions for the inner and the outer leaflets are -1.19% and 2.25%, correspondingly. As a result of the translocation of 1.4% of the outer leaflet lipids to the inner leaflet (relative to the original "state 1"), the inner leaflet actually becomes compressed even though the membrane as a total is still expanded. The free energy in "state 2" relative to a planar bilayer is 1408.8 kT, of which 27.3 kT is stretching/compression energy and 1381.4 kT is bending energy. As one can see, the total free energy in "state 2" is less than the free energy in "state 1" by 23.5 kT.

"Original state 3" would have the lowest free energy, but we have insufficient information about the *trans*-bilayer distribution of the lipids of interest here (DOPC/DOPE/Ch (2:1:1)) to treat this case meaningfully.

Influence of PEG

When PEG is added, vesicles aggregate. For simplicity, we assume only a pair of vesicles per aggregate. When the distance between two vesicles is less than the thickness of the PEG exclusion layer, these layers intercept each other and the total depletion volumes of the two vesicles and thus the depletion energy is reduced. This stabilizes the aggregate.

On the other hand, hydration repulsion between closely opposed membrane surfaces opposes aggregation. The minimum total energy at 10% PEG is -2.44 kT per contact (-1.22 kT per vesicle), when the distance between opposed membrane surfaces is 1.45 nm, relative to the energy of separate vesicles. The stability of an aggregate will depend on the number of vesicles in the aggregate and on the energy per vesicle. We note that the actual aggregate size ranges from 5 to 6 for 45 nm diameter vesicles (Lee and Lentz, 1997a) to >15 for 22 nm vesicles (K. Evans, personal communication). In such aggregates, there would be multiple contacts per vesicle: for two vesicles there is 1/2; for three vesicles placed in a triangle, 1; for four placed in a trigonal pyramid, 3/2; and for a very large aggregate with hexagonal vesicle packing, 3. To simplify, we calculate here the free energy of a pair of fusing vesicles relative to their energy in the dimer aggregated state.

Energy profiles for intermediate evolution: two intermediate states

Since our purpose was to test whether the stalk hypothesis was consistent with observations on PEG-mediated fusion, we have made simplifying assumptions that are consistent with the hypothesis. The first is that the initial intermediate that is formed at the point of contact of vesicles is the stalk intermediate. Since the topologies of all the intermediates that we analyze are the same, the evolution of intermediates can be viewed as a process along some ''reaction co-ordinate'', which we take as the stalk radius (r_S in Fig. 1). The energy profiles of a pair of SUVs as a function of the stalk radius relative to ''original state 1'' (*solid line*) and ''original state 2'' (*dashed line*) in the presence of 10% PEG are presented in Fig. 3. For both original states, the free energy of the stalk intermediate is actually slightly lower
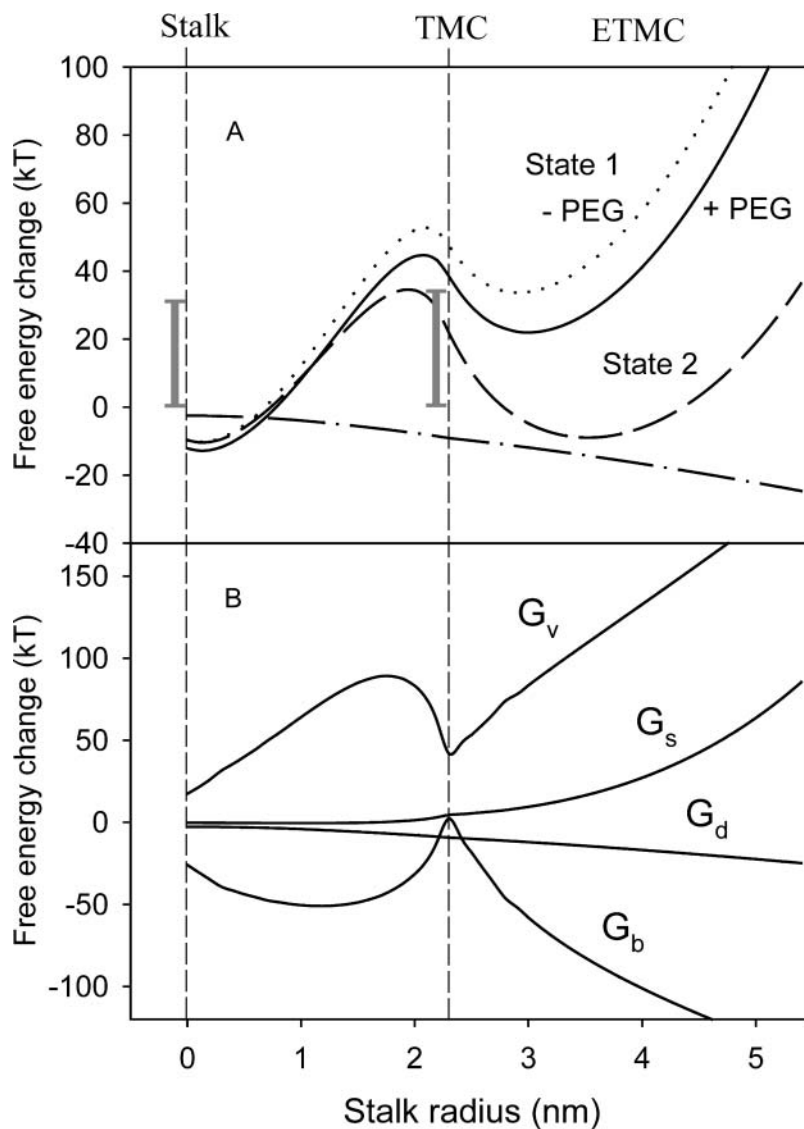

FIGURE 3 (*A*) Role of the original state in defining the free-energy profiles for fusing 26 nm vesicles. Calculated free energies of a fusing vesicle pair are presented as a function of stalk radius relative either to original state 1 (relaxation by vesicle radius change, *solid line*) or to original state 2 (as in state 1 plus lipid redistribution between leaflets, *dashed line*). Both calculations presumed the presence of 10 wt % PEG. The calculated free energy relative to state 1 in the absence of PEG is shown as a dotted line. The effect of PEG (difference between *solid* and *dotted lines*) is shown as a dot-dashed line. Experimental estimates of activation free energies for formation of the first (31 kT) and second (34 kT) intermediates in 45 nm vesicles (Lentz and Lee, 1999) are shown as vertical bars for comparison. (*B*) Major individual energy components in the total free-energy change relative to state 1 (*solid line* in *A*). G_b, bending energy; G_v, lamellar/nonlamellar mismatch or ''void'' energy; G_s, membrane stretching/compression energy; and G_d, depletion energy.

than that of the aggregated vesicles. This is because the stalk geometry relieves some of the curvature stress of the SUVs. This does not mean that the energy barrier for stalk formation is small, since this barrier is associated with a topologically discontinuous process that we cannot model by our methods. A shaded bar in Fig. 3 *A* shows an experimental estimate for the free activation energy associated with this process (Lentz and Lee, 1999). The existence of two minima in this free-energy profile is consistent with a previous report demonstrating two intermediates associated with PEG-mediated fusion of sonicated vesicles (Lee and Lentz, 1997a). Our calculation reveals a free-energy barrier between the stalk and TMC that is ~40 kT. The second shaded bar shows that an experimental estimate for this barrier (Lentz and Lee, 1999) is comparable to our calculated barrier, arguing for the reasonableness of our model.

We also show as a dotted curve in Fig. 3 *A* the free-energy profile for evolution of fusion intermediates in the absence of PEG. We assume that vesicles are brought together to a distance of 1.45 nm, the same distance that we have shown above for aggregation induced by 10% PEG. As expected, the free-energy profile in this case is higher, with the activation energy for conversion of the first to the second intermediate also increased. The difference between the free-energy profiles in the presence and absence of PEG, shown in Fig. 1 as a dot-dashed line, represents the contribution of depletion energy and clearly indicates that PEG does drive the progression of intermediates toward fusion. However, the PEG contribution is not very large compared to other energy components, and our results would be qualitatively the same if different agents induced aggregation. Overall, the free-energy profile exhibits two metastable intermediate states with local energy minima. Qualitatively it reflects mostly the changes in the void free-energy term, which has minimum volume at the stalk and TMC intermediates.

Contributions of the principal individual energy terms to the total free energy of fusion intermediates relative to the energies in "original state 1" are presented in Fig. 3 *B*. Bending energy and "void" energy clearly dominate, at least until the extended TMC is formed, at which point the stretching/compression energy rises. As expected, the bending free energy favors formation of an initial fusion intermediate, and the "void" energy is the principal term opposing formation of this intermediate and its expansion to the second intermediate or to a fusion pore. In this view, the three major barriers to fusion are: 1), the activation free energy of initial intermediate formation, 2), the "void" and bending energies that dominate intermediate progression, and 3), the activation energy of pore formation. Because the first and last contributions involve discontinuous changes in microscopic lipid topology that are not treatable with the macroscopic or materials models we adopt here, we focus in this article on understanding how environmental factors might affect intermediate progression.

Since the bending and "void" energies dominate the total intermediate free energy, and these are determined by the membrane intrinsic curvature (C_o) and specific "void" energy coefficient (K_v), we have analyzed how changes in these values affect the free-energy profile for fusion intermediate evolution (Fig. 4). As expected, the free-energy profile changed dramatically with changing K_v (Fig. 4 *A*), such that a 28% decrease in K_v (*two curves down* from *solid line* in Fig. 4 *A*) produced a situation in which the TMC intermediate is predicted to be stable relative to the aggregated, unfused state. Further decrease in K_v (43%; *lowest curve* in Fig. 4 *A*) produced a situation in which the TMC is as stable as the initial intermediate. Clearly, addition of a membrane component that can help fill hydrophobic space at the interface between lamellar and nonlamellar regions of fusing bilayers is expected to have a dramatic influence on fusion. Indeed, the addition to DOPC/DOPE/ sphingomyelin/CH SUVs of 5 mol % hexadecane, which is thought to serve this role (Walter et al., 1994), produced an
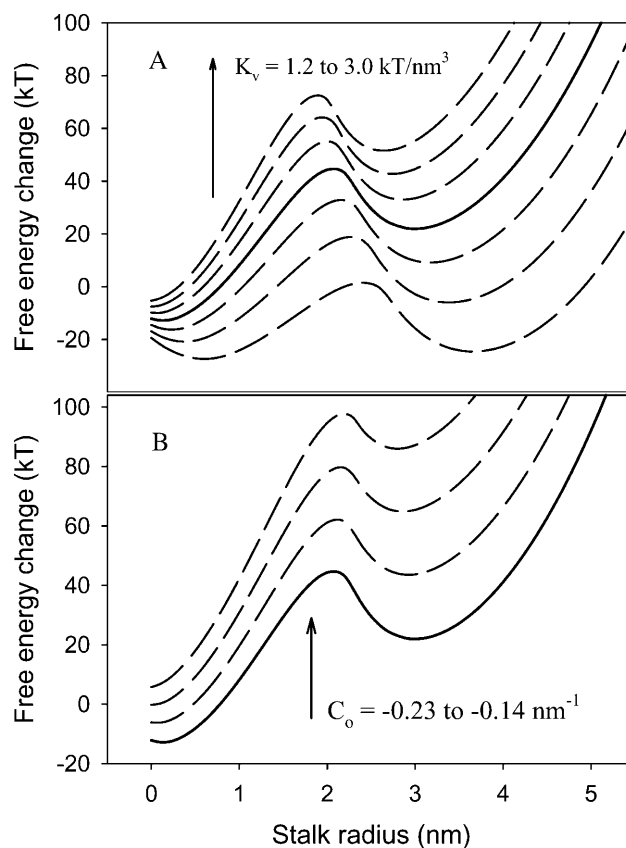

FIGURE 4 Effects of void modulus K_v (*A*) and membrane intrinsic curvature C_o (*B*) on fusion free-energy profiles. Free-energy profiles are as presented in Fig. 3. (*A*) K_v was increased from 1.2 to 3.0 kT/nm^3 from bottom to top in steps of 0.3 kT/nm^3. (*B*) C_o was increased from -0.23 to -0.14 nm^{-1} from bottom to top in steps of 0.03 nm^{-1}. The solid lines represent free-energy profiles obtained with default parameters used in most calculations in this study (K_v 2.1 kT/nm^3 and C_o -0.23 nm^{-1}).

~10-fold increase in the rate of intervesicle contents mixing (Haque and Lentz, 2002), consistent with this prediction.

The dramatic effect of membrane intrinsic curvature is shown in Fig. 4 *B*. It has previously been reported that negative intrinsic curvature can dramatically reduce the bending energy of a stalk intermediate relative to a planar membranes (Kozlovsky and Kozlov, 2002; Markin and Albanesi, 2002), so this result is not unexpected for fusing vesicles. Increasing C_o from the value we have estimated for highly fusogenic DOPC/DOPE/Ch (*bottom curve* in Fig. 4 *B*) to that expected for DOPC (*top curve*) leads to a situation in which the TMC or extended TMC structures are predicted to be quite unstable relative to the stalk. We note that another very recent calculation of the free energy of the extended TMC between planar membranes predicts that this structure would not have a free-energy minimum except for C_o between -0.2 and -0.3 nm^{-1} (Kozlovsky et al., 2002). Although this agrees qualitatively with our result, the different quantitative predictions likely reflect the different geometries assumed for the two calculations (curved and closed membrane vesicles versus open and planar membranes (Kozlovsky et al., 2002)). Since fusion-pore formation likely occurs at least in part from the TMC or extended TMC (see ''Pore formation'', below), we would expect very little fusion for vesicles with C_o of -0.14 nm^{-1} but adequate fusion with C_o of -0.23 nm^{-1}, as we have found for PEG-mediated fusion of SUVs of these limiting compositions (Malinin et al., 2002; Talbot et al., 1997).

Variation of intermediate geometry during vesicle fusion

Before addressing how environmental factors affect intermediate progression, we must examine the geometric aspects of our model. The geometry of the vesicle fusion intermediates we consider is established by four parameters: R, r_S, r_m, and r_d (see Fig. 1). r_S is the reaction coordinate for intermediate evolution. The other three geometric parameters (R, r_m, and r_d) were found by minimizing the total free energy of the system for each value of r_S. The resulting variation of two of these parameters with r_S is shown in Fig. 5 *A*. A new geometric parameter must be defined once a TMC appears. This is the radius of the contacting area of the opposite *trans*-monolayers, r_c. The beginning of the ''r_c'' curve indicates the establishment of the initial TMC intermediate. The values obtained for these parameters produce the consequence that the inner (or distal) leaflets expand during intermediate maturation while the outer (or contacting) leaflets contract (Fig. 5 *B*). If lipids cannot redistribute between leaflets during intermediate maturation, this produces a positive contribution to the stretching free energy (ΔG_S, Eq. 2). Although not as large a contribution to the total free energy as the bending and ''void'' terms, the stretching free energy does play an important role in
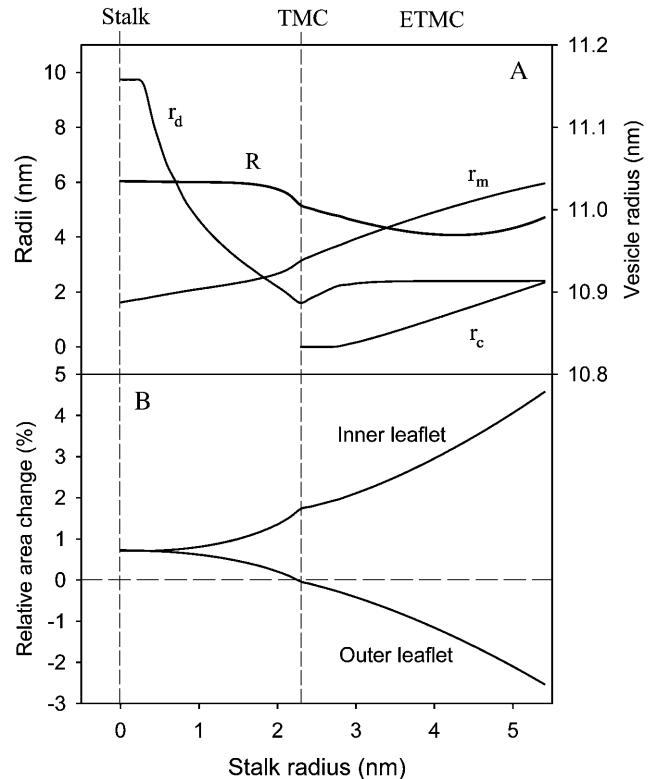

FIGURE 5 Variation in intermediate geometry during intermediate evolution. As described in the text, vesicle and intermediate geometries were allowed to vary so as to minimize the system free energy at each value of r_s. (*A*) Variation with r_s of the parameters: R (vesicle radius; *right ordinate*), r_d (dimple radius; *left ordinate*), r_m (marginal radius; *left ordinate*), and r_c (radius of the transmembrane contact area; *left ordinate*). (*B*) Variation of inner and outer leaflet relative areas with r_s.

understanding the influence of osmotic forces on intermediate evolution, as described next.

Effects of osmotic stress

Osmotic compression ($\Delta\Pi < 0$) or expansion ($\Delta\Pi > 0$) might affect fusion by changing membrane tension in ways that oppose or favor the changes in inner or outer leaflet areas associated with stalk expansion (Fig. 5 *B*). Direct calculations suggest that this effect is too small to make a significant change in the fusion profile (Fig. 6 *A*). Neither compression (*dashed curve*) nor expansion (*dash-dotted curve*) significantly altered the energy profile of fusion intermediate progression relative to a situation with $\Delta\Pi = 0$ (*solid line*), despite the fact that these calculations assumed significant osmotic forces ($\Delta\Pi = \pm 5$ atm). Nonetheless, we have observed experimentally a clear effect of osmotic stress on fusion, most notably in the late stages of fusion, with compression promoting and expansion inhibiting fusion (Malinin et al., 2002). To explain this, we hypothesized that lipid ''material'' (not necessarily individual lipid molecules) might move out of the plane of vesicle leaflets and at least
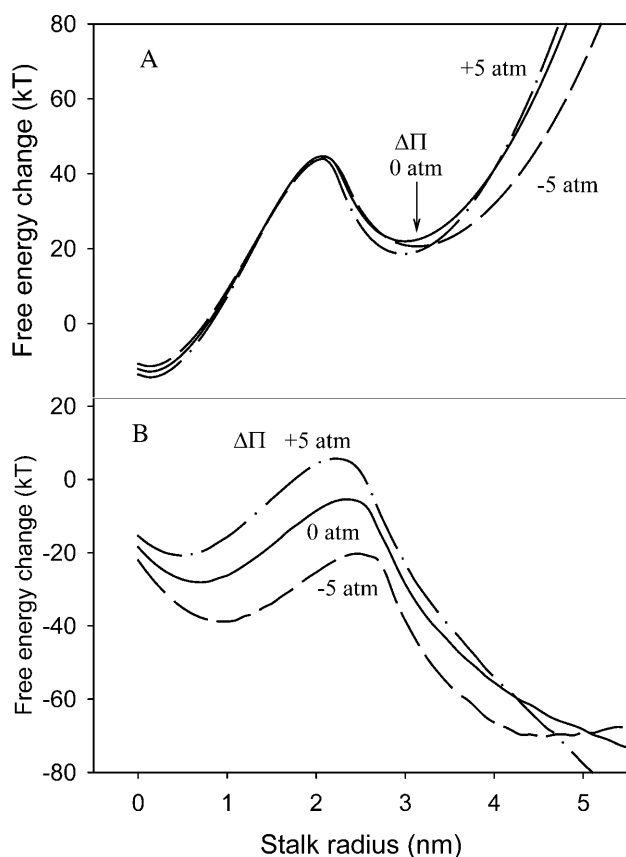
FIGURE 6 Effect of osmotic gradient. (*A*) Variation of fusing vesicle pair free energy with stalk radius for the model without lipid redistribution and for three osmotic conditions: no osmotic gradient across the vesicle membrane (*solid line*), hyperosmotic ($\Pi_{in} > \Pi_{out}$) gradient of +5 atm (*dot-dashed line*), and hypoosmotic gradient of −5 atm (*dashed line*). (*B*) As in *A*, except for the model that allows for lipid mass movement out of the bilayer leaflets and into the "void" region. Parameters of the calculation are described in the text. Osmotic gradients correspond to pressure created by adding ~200 mM sucrose inside (+) or outside (−) of vesicles.

partially fill regions of hydrophobic mismatch to reduce "void" energy. If so, osmotic gradients might help to press lipid material from the outer or inner leaflet toward the "void" (compressive gradient) or from the "void" toward the outer leaflet (swelling gradient). V_1 and V_2 represent the volumes of lipid material assumed to be moved out of the inner and outer leaflets into the "void", respectively, under the influence of a compressive osmotic gradient. Negative values of V_1 and V_2 indicate lipid material moving out of the "void" into the outer or inner leaflets under the influence of an expansive gradient.

The void coefficient, K_v, provides the energy of the packing stress introduced in lamellar regions to accommodate the hydrophobic mismatch volume. This coefficient is determined from lamellar-hexagonal phase transition experiments performed under conditions of no excess tension. Enclosed fusing vesicles can experience high tension when subjected to extreme osmotic conditions. Clearly, this tension will affect the energy of distortion of the lamellar lipid

packing surrounding hydrophobic mismatch regardless of the actual structure of the mismatch region or the molecular mechanism by which mismatch is accommodated (chain stretching, lipid tilting, hydrophobic lipid (e.g., cholesterol) redistribution into "void"). Lipid material moved into the "void" was assumed to reduce the void free energy (G_v) by reducing the void coefficient (K_v), whereas lipid material that moved out of the "void" would have the opposite effect. We also assumed that the change in void coefficient was proportional to the volume of lipid material moved into or out of the void, thus making a new void coefficient

$$K_v^* = K_v - \Delta k (V_1 + V_2)/V_v, \qquad (10)$$

where Δk is the reduction of the void energy per unit volume of lipid material transferred. With these definitions, the new void energy is still given as in Eq. 6 but with a reduced void modulus, K_v^*, replacing K_v.

This formulation allows us to parameterize the effect of osmotic tension using the corresponding volumes, V_1 and V_2, to quantitatively account for this effect. First, Eq. 10 provides for a reduction of total free energy associated with tension-induced movement of lipid material into the "void". Second, tension-induced lipid movement should also contribute to the total free energy by altering the stretching/bending energies. Removing any volume of lipid from a monolayer reduces the monolayer's original unstressed area

$$A_o^* = A_o - (V_1 + V_2)/h, \qquad (12)$$

where h is the thickness of a monolayer, and A_o and A_o^* are, respectively, the areas of an unstressed monolayer in the absence and presence of lipid movement into the "void". This reduction in area per lipid leads to changes in stretching and bending energy according to Eqs. 2 and 4.

We note that, in essence, the current model treats the "void" as a separate phase that exchanges material with the lamellar phase. Although the "void" is an imaginary construct and may not be a phase, the model has the effect of decreasing/increasing the volume of the "void" at the expense of lipid packing within the lamellar phase. We believe that, although not describing a true phase-equilibrium, this model catches the essence of the effect of osmotic stress.

Using this additional energy term and conditions for the "void" volume and leaflet area, we minimized the free energy at each r_S by varying the three geometrical parameters R, r_m, and r_d, plus volumes V_1 and V_2. To choose the appropriate value for the coefficient Δk, we performed a series of calculations fixing it at different values. We found that, if Δk was <0.5 kT/nm^3, filling "void" only slightly affected intermediate energies both with and without osmotic stress. If Δk was >1.5 kT/nm^3, the minimization became unstable, ending up in accumulation of most of the lipids in a giant void. Thus we chose $\Delta k = 1$ kT/nm^3, which

physically means that transferring 1 unit of lipid volume (1 nm^3 or ~1 lipid molecule) into the void reduces the void energy by ~1 kT.

The free-energy profile for this model is shown in Fig. 6 B. In the context of this model, osmotic stress has a remarkable effect. Specifically, vesicle expansion under a positive osmotic gradient of +5 atm increased the energy barrier between the stalk and TMC by ~4 kT and the absolute value of the barrier by ~7 kT, whereas compression both stabilized the stalk intermediate and decreased the barrier to nearly the same extents. Interestingly, it did not change much the energy of a stalk at zero radius, and this implies that it would not very much affect the barrier for stalk formation. Experimentally, we have observed that osmotic gradients affected only contents mixing of SUVs but not lipid mixing and that the effect of a compressive (negative) gradient was to promote fusion whereas that of an expansive (positive) gradient was to inhibit fusion (Malinin et al., 2002). At the time, these observations seemed quite counterintuitive, although they now find a simple explanation in terms of the idea that lipid molecules can and must distort from their shapes in lamellar structures to accommodate the packing mismatch that necessarily accompanies fusion intermediates. Osmotic stress can either impair or promote the necessary distortions that move lipid material into the "void".

The variation of V_1 and V_2 with stalk radius is given in Fig. 7 and shows how each leaflet provides lipid mass to lower "void" volume even under isoosmotic conditions (*solid line*). The left-hand ordinate in Fig. 7 shows the transferred volumes as percents of total lipid volume, whereas the right ordinate shows the absolute volume transferred. The direction of lipid material movement changes as the stalk expands and with the presence and sign of an osmotic gra-
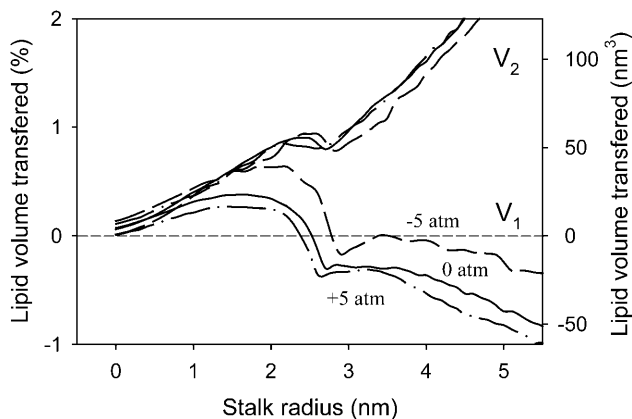

FIGURE 7 Extent of lipid redistribution. Volumes of lipid mass transferred (absolute volume on *right ordinate*, and relative to total lipid volume on *left ordinate*) to the "void" from inner (V_1) and outer (V_2) leaflet to minimize the system free energy at each value of r_S. Negative values of V_1 at $r_S > 2.3$ nm indicate that lipid mass moves back to the inner leaflet, thus making the net movement from the outer to the inner leaflet. Local variations within the curve reflect the difficulty of determining precise free-energy minima with respect to V_1 and V_2, especially for $r_S > 2.3$ nm.

dient. When the initial stalk intermediate is first formed, lipids move from both leaflets to a nearly equal extent to compensate for the "void". As the stalk expands toward a TMC, the movements of lipid mass from the inner (V_1) and outer (V_2) leaflets into the "void" diverge significantly. Later, when the initial stalk intermediate converts to the TMC intermediate, most of the lipid material needed to lower the large void energy comes from the outer leaflet (V_2), independent of the direction of the osmotic gradient. However, movement of lipid material between the "void" and the inner leaflet (V_1) is quite different depending on the sign of the osmotic gradient. For no or positive osmotic gradients, material actually moves out of the "void" and into the inner leaflet. This accounts for the higher intermediate free energy and the decrease in pore formation seen for osmotically swollen vesicles (Malinin et al., 2002). On the other hand, a compressive or negative osmotic gradient limits the amount of material flow from the "void" into the inner leaflet, accounting for the positive influence of a compressive gradient on pore formation (Malinin et al., 2002). To understand why a compressive gradient would have this effect, one must remember that the pressure gradient is felt on all membranes that delimit the interior and exterior compartments but is not felt on the membrane (septum) that delimits the two, trapped compartments. The result is that, whatever the effect of the osmotic gradient on the vesicle membrane, it has the opposite effect on the septum membrane.

Effect of vesicle curvature

We report elsewhere that high membrane curvature induced by mechanical stress (i.e., sonication) promotes pore formation while not having a significant effect on the rate of formation of the initial intermediate (Evans and Lentz, 2002; Malinin et al., 2002). This is surprising, since we have in the past interpreted the increase of fusion with curvature as due to destabilization of vesicle outer leaflets in highly curved membranes (Lee and Lentz ,1997b; Talbot et al., 1997). We now ask, in terms of the model developed here, how increasing membrane curvature affects the evolution of fusion intermediates. Fig. 8 A shows free-energy profiles of fusing vesicles of increasing radii from 11 nm (*bottom*) to 200 nm (*top*). We note a dramatic increase in the energy barrier between the stalk and TMC intermediates as vesicle diameter increases and curvature decreases. The energy barrier between the stalk and TMC intermediates decreased roughly linearly with the reciprocal of vesicle radius (membrane curvature) (Fig. 9). This is consistent with the observation that fusion increased with decreasing vesicle diameter (Talbot et al., 1997).

Lipid redistribution and fusion

Among the insights we have obtained from this study is the potential importance of lipid redistribution to fusion. We
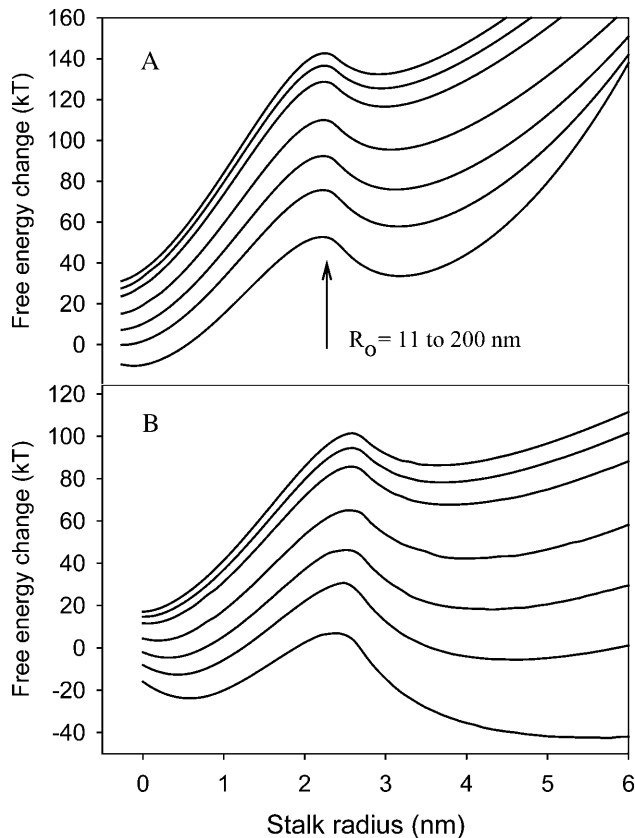
FIGURE 8 Effect of membrane curvature on the free-energy profile of fusing vesicles. Vesicle radii were 11, 15, 20, 30, 60, 100, and 200 nm in the order from bottom to top. (*A*) Standard model without lipid redistribution. (*B*) Model with lipid redistribution allowed.
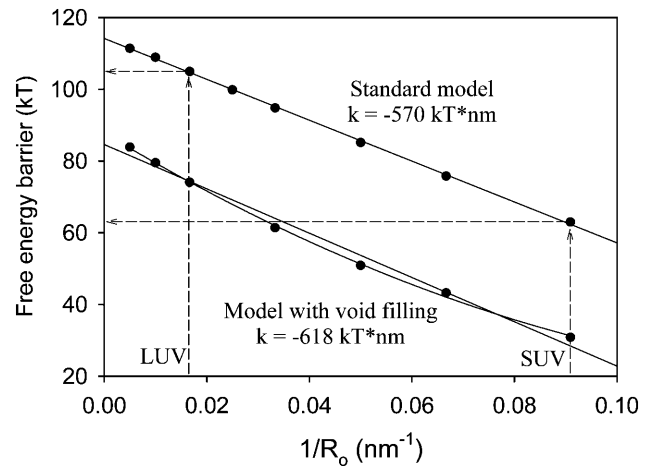

FIGURE 9 Dependence of the free-energy barrier between the first and the second intermediate on vesicle curvature. The free-energy barrier is plotted versus reciprocal of vesicle radius (membrane curvature) for the standard model (no lipid redistribution, *upper curve*) and the lipid redistribution model (*lower curve*), with linear regression coefficients shown.

considered the effects of two types of lipid redistribution. One of these is redistribution between outer and inner leaflets during formation of SUVs. We have estimated that this redistribution can lower the free energy of unfused ''state 2'' vesicles by nearly 24 kT relative to unrelaxed ''state 1'' vesicles (Fig. 3 *A*). ''State 2'' vesicles also have a lower activation energy for formation of an ETMC intermediate, and this intermediate is more stable at higher stalk radii than seen with ''state 1'' vesicles (Fig. 3 *A*). We consider in the next section what this might mean in terms of fusion.

The second type of lipid redistribution occurs during formation of fusion intermediates to lower the effective ''void''. Our calculations estimate only the effect of moving mass into the region of nonlamellar structure associated with fusion intermediates and out of the leaflets of the fusing vesicles. This movement could take the form of lipid acyl chain stretching, of creation of membrane surface defects, or of *trans*-bilayer lipid migration. The latter would be consistent with our calculations suggesting that net movement from the outer to the inner leaflet would favor TMC formation and expansion to create a pore (Fig. 7). This is consistent with observations showing that this net movement of lipids does indeed occur on the timescale of the slower of

two detectable lipid redistribution processes observed during PEG-mediated fusion (Evans and Lentz, 2002).

We note that our treatment of lipid movement ignores potentially important processes such as preferential *trans*-bilayer or in-plane redistribution of certain lipid classes or species. We did not study either scenario in our calculations, though we modeled membranes composed of three different species, DOPC, DOPE, and cholesterol. This nonrandom distribution of lipid could have profound consequences for fusion, since even these three lipids vary considerably in their intrinsic curvatures and thus could dramatically affect the stability of fusion intermediates. However, such an analysis, even in its simplest form, would require too many new parameters in addition to the five used for modeling lipid mass transfer. Without additional observations with which to limit the possible values of these parameters, such a calculation would be meaningless.

Pore formation

Calculations based on macroscopic material properties of lipid phases cannot shed light on the processes leading to formation of a stalk intermediate or conversion of an intermediate state to a pore, since these events involve discontinuous changes in the topology of aggregated lipid states. However, simulations of stochastic events based on molecular or simple particle potentials can be reasonably used to explore these discontinuous events. Particle dynamics simulations suggest that fusion pore formation occurs at the strained edges of either the stalk or TMC intermediate (Muller et al., 2002; Noguchi, 2002; Noguchi and Takasu, 2001), although pores can form in some instances at the center of highly curved contacts between

bilayers (Marrink and Tieleman, 2002; Noguchi and Takasu, 2001). It stands to reason that fusion intermediate instability and the probability of pore formation will increase in proportion to: 1), the probability of finding the system in a given intermediate, 2), the amount of lipid in the torroidal boundary of the intermediate, and 3), the packing stress in the intermediate boundary. The amount of torroidal boundary clearly is greatest in the ETMC structure. Packing stress should reflect both bending energy, which is maximal at the TMC (Fig. 3 *B*), as well as the ''void'' free energy, which has a local maximum for a dimpled or slightly expanded stalk, a minimum at the TMC, and then increases without bound as the TMC expands (Fig. 3 *B*). From these considerations, we might expect pore formation to be possible but still unlikely for a slightly expanded stalk (dimpled stalk in Fig. 1) but most likely in a TMC or slightly expanded TMC. A recent treatment of the ETMC from a materials perspective suggests that pore formation might be optimal at the strained edge of the ETMC structure (Kozlovsky et al., 2002), although, unlike conclusions based on stochastic models, this conclusion is based on the assumption of certain geometries.

Experiment is consistent with the possibility that pore formation could take place in either of the intermediate structures. Thus, we and others have observed two types of pores, an initial pore of limited permeability and transient duration (Chanturiya et al., 1997; Lee and Lentz, 1997a) or a more substantial but more slowly forming pore that we have termed the fusion pore (Lee and Lentz, 1997a). Our calculations suggest that conditions that favor formation of a stable and expandable ETMC will promote fusion pore formation. Both membrane curvature and a negative osmotic gradient are predicted to favor ETMC formation and expansion (Figs. 8 and 9, and 6 and 7) and both are observed (Evans and Lentz, 2002; Malinin et al., 2002) to promote fusion pore formation.

It should be noted that ETMC structures have not been observed in stochastic simulations except when some force exists to drive formation of an uncurved bilayer (Noguchi, 2002). However, the particle potentials that lead to this observation are very crude, so it is unclear whether such a conclusion might be altered by more accurate calculations taking into account such effects as intrinsic lipid curvature, osmotic stress across bilayers, or the presence of PEG or fusion proteins driving close membrane contact. This is a significant issue that deserves further exploration by dynamics simulations.

SUMMARY

This work was initiated to ask whether the unexpected effects of osmotic gradients and high membrane curvature on PEG-mediated fusion (Evans and Lentz, 2002; Malinin et al., 2002) might be interpretable in terms of the stalk model of the fusion process. Although limited to those steps of the fusion process that can reasonably be modeled in terms of the material properties of lipid assemblies, our quantitative treatment has made predictions that are consistent with observation. Overall, the results support the stalk hypothesis and suggest that fusion pore formation should be promoted by membrane components or conditions that can minimize the packing mismatch (''void'') between lamellar and nonlamellar structures involved in fusion intermediates.

REFERENCES

Arnold, K., O. Zschoernig, D. Barthel, and W. Herold. 1990. Exclusion of poly(ethylene glycol) from liposome surfaces. *Biochim. Biophys. Acta.* 1022:303–310.

Bentz, J. 2000. Membrane fusion mediated by coiled coils: a hypothesis. *Biophys. J.* 78:886–900.

Bonnafous, P., and T. Stegmann. 2000. Membrane perturbation and fusion pore formation in influenza hemagglutinin-mediated membrane fusion. A new model for fusion. *J. Biol. Chem.* 275:6160–6166.

Chanturiya, A., L. V. Chernomordik, and J. Zimmerberg. 1997. Flickering fusion pores comparable with initial exocytotic pores occur in protein-free phospholipid bilayers. *Proc. Natl. Acad. Sci. USA.* 94:14423–14428.

Chen, Z., and R. P. Rand. 1997. The influence of cholesterol on phospholipid membrane curvature and bending elasticity. *Biophys. J.* 73:267–276.

Chernomordik, L. V., and J. Zimmerberg. 1995. Bending membranes to the task: structural intermediates in bilayer fusion. *Curr. Opin. Struct. Biol.* 5:541–547.

do Carmo, M. 1976. Differential Geometry of Curves and Surfaces. Prentice-Hall, Englewood Cliffs, NJ.

Evans, E., and D. Needham. 1987. Physical properties of surfactant bilayer membranes: thermal transitions, elasticity, rigidity, cohesion, and colloidal interactions. *J. Phys. Chem.* 91:4219–4228.

Evans, K. O., and B. R. Lentz. 2002. Kinetics of lipid rearrangements during poly(ethylene glycol)-mediated fusion of highly curved unilamellar vesicles. *Biochemistry.* 41:1241–1249.

Fuller, N., and R. P. Rand. 2001. The influence of lysolipids on the spontaneous curvature and bending elasticity of phospholipid membranes. *Biophys. J.* 81:243–254.

Hamm, M., and M. M. Kozlov. 1998. Tilt model of inverted amphiphilic mesophases. *Eur. Phys. J. B.* 6:519–528.

Haque, M. E., and B. R. Lentz. 2002. Influence of gp41 fusion peptide on the kinetics of poly(ethylene glycol)-mediated model membrane fusion. *Biochemistry.* 41:10866–10876.

Helfrich, W. 1973. Elastic properties of lipid bilayers: theory and possible experiments. *Z. Naturforsch.* 28:693–703.

Israelachvili, J., and R. Pashley. 1982. The hydrophobic interaction is long range, decaying exponentially with distance. *Nature.* 300:341–342.

Kanaseki, T., K. Kawasaki, M. Murata, Y. Ikeuchi, and S. Ohnishi. 1997. Structural features of membrane fusion between influenza virus and liposome as revealed by quick-freezing electron microscopy. *J. Cell Biol.* 137:1041–1056.

Kirk, G. L., S. M. Gruner, and D. L. Stein. 1984. A thermodynamic model of the lamellar to inverse hexagonal phase-transition of lipid-membrane water-systems. *Biochemistry.* 23:1093–1102.

Kozlov, M. M., and L. V. Chernomordik. 1998. A mechanism of protein-mediated fusion: coupling between refolding of the influenza hemagglutinin and lipid rearrangements. *Biophys. J.* 75:1384–1396.

Kozlov, M. M., S. Leikin, and R. P. Rand. 1994. Bending, hydration, and interstitial energies quantitatively account for the hexagonal-lamellar-hexagonal reentrant phase-transition in dioleoylphosphatidyletanolamine. *Biophys. J.* 67:1603–1611.

Kozlov, M. M., and M. Winterhalter. 1991. Elastic-moduli for strongly curved monolayers—position of the neutral surface. *J. Phys. II.* 1:1077–1084.

Kozlovsky, Y., L. V. Chernomordik, and M. M. Kozlov. 2002. Lipid intermediates in membrane fusion: formation, structure, and decay of hemifusion diaphragm. *Biophys. J.* 83:2634–2651.

Kozlovsky, Y., and M. M. Kozlov. 2002. Stalk model of membrane fusion: solution of energy crisis. *Biophys. J.* 82:882–895.

Kuhl, T., Y. Q. Guo, J. L. Alderfer, A. D. Berman, D. Leckband, J. Israelachvili, and S. W. Hui. 1996. Direct measurement of polyethylene glycol induced depletion attraction between lipid bilayers. *Langmuir.* 12:3003–3014.

Kuzmin, P. I., J. Zimmerberg, Y. A. Chizmadzhev, and F. S. Cohen. 2001. A quantitative model for membrane fusion based on low-energy intermediates. *Proc. Natl. Acad. Sci. USA.* 98:7235–7240.

Lee, J., and B. R. Lentz. 1997a. Evolution of lipidic structures during model membrane fusion and the relation of this process to cell membrane fusion. *Biochemistry.* 36:6251–6259.

Lee, J., and B. R. Lentz. 1997b. Outer leaflet-packing defects promote poly(ethylene glycol)-mediated fusion of large unilamellar vesicles. *Biochemistry.* 36:421–431.

Leikin, S., M. M. Kozlov, N. L. Fuller, and R. P. Rand. 1996. Measured effects of diacylglycerol on structural and elastic properties of phospholipid membranes. *Biophys. J.* 71:2623–2632.

Leikin, S. L., M. M. Kozlov, L. V. Chernomordik, V. S. Markin, and Y. A. Chizmadzhev. 1987. Membrane fusion: overcoming of the hydration barrier and local restructuring. *J. Theor. Biol.* 129:411–425.

Lentz, B. R., T. J. Carpenter, and D. R. Alford. 1987. Spontaneous fusion of phosphatidylcholine small unilamellar vesicles in the fluid phase. *Biochemistry.* 26:5389–5397.

Lentz, B. R., and J. K. Lee. 1999. Poly(ethylene glycol) (PEG)-mediated fusion between pure lipid bilayers: a mechanism in common with viral fusion and secretory vesicle release? *Mol. Membr. Biol.* 16:279–296.

Lentz, B. R., V. Malinin, M. E. Haque, and K. Evans. 2000. Protein machines and lipid assemblies: current views of cell membrane fusion. *Curr. Opin. Struct. Biol.* 10:607–615.

Lentz, B. R., G. F. McIntyre, D. J. Parks, J. C. Yates, and D. Massenburg. 1992. Bilayer curvature and certain amphipaths promote poly(ethylene glycol)-induced fusion of dipalmitoylphosphatidylcholine unilamellar vesicles. *Biochemistry.* 31:2643–2653.

Lentz, B. R., D. P. Siegel, and V. Malinin. 2002. Filling potholes on the path to fusion pores. *Biophys. J.* 82:555–557.

Lis, L. J., M. McAlister, N. Fuller, R. P. Rand, and V. A. Parsegian. 1982. Interactions between neutral phospholipid bilayer membranes. *Biophys. J.* 37:657–665.

Malinin, V., and B. R. Lentz. 2004. On the analysis of osmotic stress in hexagonal phases. *Biophys. J.* 86:3324–3328.

Malinin, V. S., P. Frederik, and B. R. Lentz. 2002. Osmotic and curvature stress affect PEG-induced fusion of lipid vesicles but not mixing of their lipids. *Biophys. J.* 82:2090–2100.

Markin, V. S. 1981. Lateral organization of membranes and cell shapes. *Biophys. J.* 36:1–19.

Markin, V. S., and J. P. Albanesi. 2002. Membrane fusion: stalk model revisited. *Biophys. J.* 82:693–712.

Markin, V. S., M. M. Kozlov, and V. L. Borovjagin. 1984. On the theory of membrane fusion. The stalk mechanism. *Gen. Physiol. Biophys.* 3:361–377.

Marra, J., and J. Israelachvili. 1985. Direct measurements of forces between phosphatidylcholine and phosphatidylethanolamine bilayers in aqueous electrolyte solutions. *Biochemistry.* 24:4608–4618.

Marrink, S. J., and D. P. Tieleman. 2002. Molecular dynamics simulation of spontaneous membrane fusion during a cubic-hexagonal phase transition. *Biophys. J.* 83:2386–2392.

Marsh, D. 1996. Intrinsic curvature in normal and inverted lipid structures and in membranes. *Biophys. J.* 70:2248–2255.

May, S. 2002. Structure and energy of fusion stalks: the role of membrane edges. *Biophys. J.* 83:2969–2980.

McIntosh, T. J., S. Advani, R. E. Burton, D. V. Zhelev, D. Needham, and S. A. Simon. 1995. Experimental tests for protrusion and undulation pressures in phospholipid bilayers. *Biochemistry.* 34:8520–8532.

Muller, M., K. Katsov, and M. Schick. 2002. New mechanism of membrane fusion. *J. Chem. Phys.* 116:2342–2345.

Needham, D., and R. S. Nunn. 1990. Elastic deformation and failure of lipid bilayer membranes containing cholesterol. *Biophys. J.* 58:997–1009.

Noguchi, H. 2002. Fusion and toroidal formation of vesicles by mechanical forces: a Brownian dynamics simulation. *J. Chem. Phys.* 117:8130–8137.

Noguchi, H., and M. Takasu. 2001. Fusion pathways of vesicles: a Brownian dynamics simulation. *J. Chem. Phys.* 115:9547–9551.

Rand, R. P., N. Fuller, V. A. Parsegian, and D. C. Rau. 1988. Variation in hydration forces between neutral phospholipid bilayers: evidence for hydration attraction. *Biochemistry.* 27:7711–7722.

Schmidt, C. F., D. Lichtenberg, and T. E. Thompson. 1981. Vesicle-vesicle interactions in sonicated dispersions of dipalmitoylphosphatidylcholine. *Biochemistry.* 20:4792–4797.

Siegel, D. P. 1993. Energetics of intermediates in membrane fusion: comparison of stalk and inverted micellar intermediate mechanisms. *Biophys. J.* 65:2124–2140.

Siegel, D. P. 1999. The modified stalk mechanism of lamellar/inverted phase transitions and its implications for membrane fusion. *Biophys. J.* 76:291–313.

Suurkuusk, J., B. R. Lentz, Y. Barenholz, R. L. Biltonen, and T. E. Thompson. 1976. A calorimetric and fluorescent probe study of the gel-liquid crystalline phase transition in small, single-lamellar dipalmitoylphosphatidylcholine vesicles. *Biochemistry.* 15:1393–1401.

Talbot, W. A., L. X. Zheng, and B. R. Lentz. 1997. Acyl chain unsaturation and vesicle curvature alter outer leaflet packing and promote poly(ethylene glycol)-mediated membrane fusion. *Biochemistry.* 36: 5827–5836.

Templer, R. H., B. J. Khoo, and J. M. Seddon. 1998. Gaussian curvature modulus of an amphiphilic monolayer. *Langmuir.* 14:7427–7434.

Turner, D. C., and S. M. Gruner. 1992. X-ray diffraction reconstruction of the inverted hexagonal (H_{II}) phase in lipid-water systems. *Biochemistry.* 31:1340–1355.

Walter, A., P. L. Yeagle, and D. P. Siegel. 1994. Diacylglycerol and hexadecane increase divalent cation-induced lipid mixing rates between phosphatidylserine large unilamellar vesicles. *Biophys. J.* 66:366–376.

Wilschut, J., N. Duzgunes, and D. Papahadjopoulos. 1981. Calcium/magnesium specificity in membrane fusion: kinetics of aggregation and fusion of phosphatidylserine vesicles and the role of bilayer curvature. *Biochemistry.* 20:3126–3133.

Yang, L., and H. W. Huang. 2002. Observation of a membrane fusion intermediate structure. *Science.* 297:1877–1879.